Eur. Phys. J. C (2020) 80:986
https://doi.org/10.1140/epjc/s10052-020-8365-0

THE EUROPEAN PHYSICAL JOURNAL C

Regular Article - Experimental Physics

Search for *CP* violation in $\Xi_c^+ \to pK^-\pi^+$ decays using model-independent techniques

LHCb Collaboration[⋆]

CH-1211, Geneva 23, Switzerland

Received: 8 June 2020 / Accepted: 8 August 2020 / Published online: 26 October 2020

Abstract A first search for *CP* violation in the Cabibbo-suppressed $\Xi_c^+ \to pK^-\pi^+$ decay is performed using both a binned and an unbinned model-independent technique in the Dalitz plot. The studies are based on a sample of proton-proton collision data, corresponding to an integrated luminosity of 3.0 fb^{-1}, and collected by the LHCb experiment at centre-of-mass energies of 7 and 8 TeV. The data are consistent with the hypothesis of no *CP* violation.

1 Introduction

The non-invariance of fundamental interactions under the combination of charge conjugation and parity transformation, known as *CP* violation (*CPV*), is a key requirement for the generation of the baryon–antibaryon asymmetry in the early Universe [1–3]. In the Standard Model (SM) of particle physics, *CPV* is included through the introduction of a single irreducible complex phase in the Cabibbo–Kobayashi–Maskawa (CKM) quark-mixing matrix [4,5]. The amount of *CPV* predicted by the CKM mechanism is not sufficient to explain a matter-dominated universe [6,7] and other sources of *CPV* are required. The realization of *CPV* in nature has been well established in the K- and B-meson systems by several experiments [8–14]. The LHCb experiment has observed for the first time *CPV* in the charm-meson sector as the difference of the *CP* asymmetries between the two-body decays $D^0 \to K^-K^+$ and $D^0 \to \pi^-\pi^+$ [15]. A similar study using Λ_c^+ to pK^-K^+ and $p\pi^-\pi^+$ found no evidence for *CPV* [16]. Indeed, so far, *CPV* has never been observed in any baryon system. Evidence for *CPV* in the b baryon sector reported by the LHCb collaboration in [17] has not been confirmed with more data [18]. Further measurements of processes involving the decay of charm hadrons can shed light on the origin and magnitude of *CPV* mechanisms within the SM and beyond.

In two-body decays of charm hadrons, *CPV* can manifest itself as an asymmetry between partial decay rates. Multi-body decays offer access to more observables that are sensitive to *CP*-violating effects. For a three-body baryon decay the kinematics can be characterised by three Euler angles and two squared invariant masses, which form a Dalitz plot [19]. The Euler angles are redundant if all initial spin states are integrated over. Interference effects in the Dalitz plot probe *CP* asymmetries in both the magnitudes and phases of amplitudes. In three-body decays there can be large local *CP* asymmetries in the Dalitz plot, even when no significant global *CPV* exists. A recent example has been measured in the decay $B^+ \to \pi^+\pi^-\pi^+$ [20].

In the SM, *CPV* asymmetries in the charm sector are expected at the order of 10^{-3} or less [21] for singly Cabibbo-suppressed (SCS) decays. New physics (NP) contributions can enhance *CP*-violating effects up to 10^{-2} [22–30]. Searches for *CPV* in Ξ_c^+ baryon decays[1] provide a test of the SM and place constraints on NP parameters [31–35]. In contrast to SCS decays, in Cabibbo-favoured (CF) charm-quark transitions, such as $\Lambda_c^+ \to pK^-\pi^+$ decays, there is only one dominant amplitude in the SM, resulting in no *CP*-violating effects. However this could change with NP, as argued above in the case of SCS decays.

This article describes searches for direct *CPV* in the SCS decay $\Xi_c^+ \to pK^-\pi^+$, for Ξ_c^+ baryons produced promptly in pp collisions. The $\Lambda_c^+ \to pK^-\pi^+$ decay is used as a control mode to study in data the level of experimental asymmetries that pollute the measurement. In this paper, the symbol H_c^+ is used to refer to both Ξ_c^+ and Λ_c^+. It is assumed that the polarisation of charm baryons produced in pp collisions is sufficiently small, as it is for b-baryons [36], to justify the integration over the Euler angles. This measurement uses pp collision data, corresponding to an integrated luminosity of 3 fb^{-1}, recorded by the LHCb detector in 2011 (1 fb^{-1}) at a centre-of-mass energy of 7 TeV, and in 2012 (2 fb^{-1}) at a centre-of-mass energy of 8 TeV. The magnetic field polarity is reversed regularly during the data taking in order to min-

⋆ e-mail: lhcb.secretariat@cern.ch

[1] Unless stated explicitly, the inclusion of charge-conjugate states is implied throughout.

imise effects of charged particle and antiparticle detection asymmetries. Approximately half of the data are collected with each polarity.

There is presently no successful method for computing decay amplitudes in multi-body charm decays, which could provide reliable predictions on how the *CP* asymmetries vary over the phase space of the decay. This situation favours a model-independent approach, which looks for differences between multivariate density distributions for baryons and antibaryons. Therefore, in this article searches for *CP V* are performed through a direct comparison between the Dalitz plots of Ξ_c^+ and Ξ_c^- decays using a binned significance (S_{CP}) method [37] and an unbinned k-nearest neighbour method (kNN) [38–41], both of which are model independent.

2 Detector and simulation

The LHCb detector [42,43] is a single-arm forward spectrometer covering the pseudorapidity range $2 < \eta < 5$. It is designed for the study of particles containing b and c quarks. The detector includes a high-precision tracking system consisting of a silicon-strip vertex detector surrounding the pp interaction region, a large-area silicon-strip detector located upstream of a dipole magnet with a bending power of about 4 Tm, and three stations of silicon-strip detectors and straw drift tubes placed downstream of the magnet. The tracking system provides a measurement of the momentum, p, of charged particles with a relative uncertainty that varies from 0.5% at low momentum to 1.0% at 200 GeV/c. The minimum distance of a track to a primary vertex (PV), the impact parameter (IP), is measured with a resolution of $(15+29/p_{\mathrm{T}})\,\mu$m, where p_{T} is the component of the momentum transverse to the beam, in GeV/c. Different types of charged hadrons are distinguished using information from two ring-imaging Cherenkov detectors. Photons, electrons and hadrons are identified by a calorimeter system consisting of scintillating-pad and preshower detectors, an electromagnetic and a hadron calorimeter. Muons are identified by a system composed of alternating layers of iron and multiwire proportional chambers.

Samples of simulated events are used to optimise the signal selection, to derive the angular efficiency and to correct the decay-time efficiency. In the simulation, pp collisions are generated using PYTHIA [44] with a specific LHCb configuration [45]. Decays of hadronic particles are described by EVTGEN [46], in which final-state radiation is generated using PHOTOS [47]. The interaction of the generated particles with the detector, and its response, are implemented using the GEANT4 toolkit [48] as described in Ref. [49].

3 Selection of signal candidates

The online event selection is performed by a trigger consisting of a hardware stage, based on information from the calorimeter and muon systems, followed by two software stages. At the hardware trigger stage, events are required to have either muons with high p_{T} or hadrons, photons or electrons with a high transverse-energy deposit in the calorimeters. For hadrons, the transverse energy threshold is approximately 3.5 GeV/c^2. In the first software trigger stage at least one good-quality track with $p_{\mathrm{T}} > 300$ MeV/c is required. In the second software trigger stage an H_c^+ candidate is fully reconstructed from three high-quality tracks not pointing to any PV. The three tracks should form a secondary vertex (SV) which must be well separated from any PV. A momentum $p > 3$ GeV/c for each track and the scalar sum of p_{T} for the three tracks $p_{\mathrm{T}} > 2$ GeV/c are required. The combined invariant mass of the three tracks is required to be in the range 2190−2570 MeV/c^2. Requirements are also placed on the particle identification criteria of the tracks and on the angle between the vector from the associated PV to the SV and the H_c^+ momentum. The associated PV is the one with smallest difference in vertex fit χ^2 when performed with and without the H_c^+ candidate.

In the offline analysis, tighter selection requirements are placed on the track-reconstruction quality, the p and p_{T} of the final-state particles. For protons $10 < p < 100$ GeV/c is required, while kaons and pions momentum satisfies $3 < p < 150$ GeV/c. Only H_c^+ candidates with p_{T} in the range $4 < p_{\mathrm{T}} < 16$ GeV are retained. Additional requirements are also made on the SV fit quality, and the minimum significance of the displacement from the SV to any PV in the event. This reduces the contribution of charm baryons from b-hadron decays to less than 5% of the prompt signal. Reconstructed particles are accepted if their momenta are within a region defined by $|p_x| < 0.2\,p_z$ and $|p_x| > 0.01\,p_z$, where p_x and p_z are the momentum components along the x and z axes.[2] This requirement has a signal loss of 25%, and is imposed to avoid large detection asymmetries that are present in the excluded kinematic regions. Differences between particles and antiparticles in reconstruction efficiencies are also observed for H_c^+ candidates where $p < 20$ GeV/c for all charged tracks. These differences do not cancel by simply averaging the data acquired with opposite magnet polarities. To minimise the reconstruction asymmetry, the momentum of all tracks is required to be greater than 20 GeV/c. This requirement rejects about 20% of the selected charm-baryon candidates.

[2] The LHCb coordinate system is right-handed, with the z axis pointing along the beam axis, y the vertical direction, and x the horizontal direction. The (x, z) plane is the bending plane of the dipole magnet.

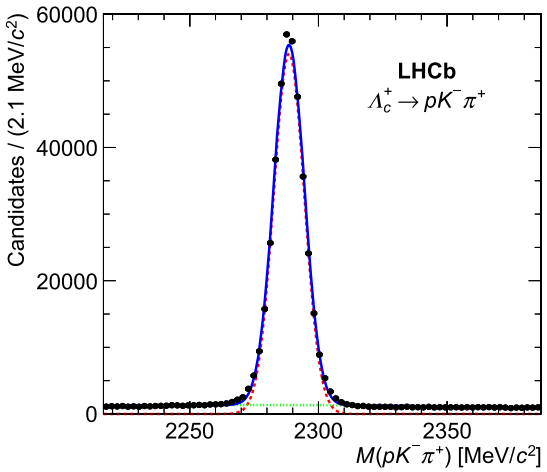

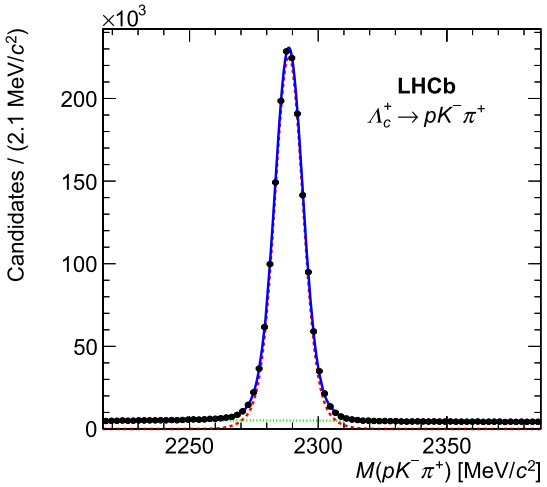

Fig. 1 Invariant-mass, $M(pK^-\pi^+)$, distributions of selected Λ_c^+ candidates are shown in the (left) 2011 and (right) 2012 data samples. Data points are in black. The overlaid fitted model (blue continuous line) is a sum of two Gaussian functions with the same mean and different widths (red dashed line) and a second-order Chebyshev polynomial function (green dotted line) describing the signal and background components

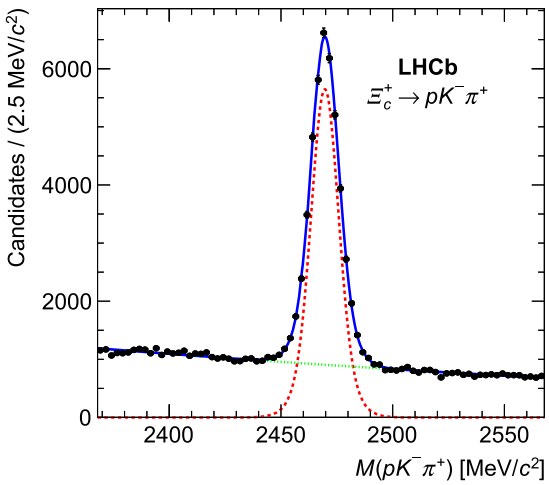

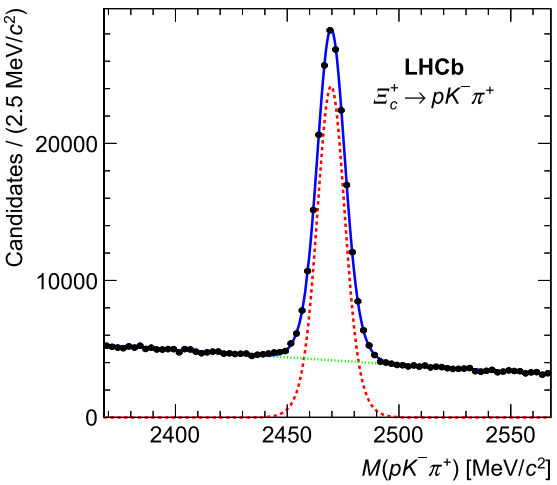

Fig. 2 Invariant-mass, $M(pK^-\pi^+)$, distributions of selected Ξ_c^+ candidates are shown in the (left) 2011 and (right) 2012 data samples. Data points are in black. The overlaid fitted model (blue continuous line) is a sum of two Gaussian functions with the same mean and different widths (red dashed line) and a second-order Chebyshev polynomial function (green dotted line) describing the signal and background components

The distributions of the invariant-mass, $M(pK^-\pi^+)$, of selected Λ_c^+ and Ξ_c^+ candidates are presented in Figs. 1 and 2, respectively, with fit curves overlaid. The fit model comprises a sum of two Gaussian functions describing the signal and a second-order Chebyshev polynomial function describing the combinatorial background. No additional source of background is found to contribute significantly, according to studies in data reconstructed with different mass hypotheses.

The final samples used for the CPV search comprise all candidates with $M(pK^-\pi^+)$ within $\pm 3\sigma$ around $m(\Lambda_c^+)$ or $m(\Xi_c^+)$, where σ is the weighted average of the two fitted Gaussian widths and $m(\Lambda_c^+)$ and $m(\Xi_c^+)$ are the masses of the Λ_c^+ and Ξ_c^+ baryons [50]. There are approximately 2.0 million Λ_c^+ candidates (0.4 million in the 2011 and 1.6 million in the 2012 data sample) and 0.25 million Ξ_c^+ candidates (0.05 million in the 2011 and 0.2 million in the 2012 data sample). The purity for Λ_c^+ decays is 94% for 2011 and 98% for 2012 and that for Ξ_c^+ decays is 77% for 2011 and 78% for 2012, where purity is defined as the number of signal candidates obtained from the fit to the invariant-mass distribution divided by the total number of candidates.

4 Methods

The Dalitz plot for $H_c^+ \to pK^-\pi^+$ is formed by the squares of the invariant masses of two pairs of the decay products: $M^2(K^-\pi^+)$ and $M^2(pK^-)$. Comparisons of the Dalitz plots

of H_c^+ and H_c^- candidates are performed using the binned S_{CP} and the unbinned kNN methods, described in the following. For both the binned S_{CP} and unbinned kNN methods, a signal of CPV is established if a p-value lower then 3×10^{-7} is found, corresponding to an exclusion of CP symmetry with a significance of five standard deviations. However, in case that no CPV is found, there is no model-independent mechanism for setting an upper limit on the amount of CPV in the Dalitz plot.

4.1 Binned S_{CP} method

The S_{CP} method [37] has been used before for searches of CPV testing in charm and beauty decays [41,51–54]. This method is used to search for localised asymmetries in the phase space of the decay $H_c^+ \to pK^-\pi^+$ and is based on a bin-by-bin comparison between the Dalitz plots of baryons, H_c^+, and antibaryons, H_c^-. The Dalitz plots of H_c^+ and H_c^- are divided using an identical binning. For each bin i of the Dalitz plot, the significance of the difference between the number of H_c^+ (n_+^i) and H_c^- (n_-^i) candidates, is computed as

$$S_{CP}^i = \frac{n_+^i - \alpha n_-^i}{\sqrt{\alpha(n_+^i + n_-^i)}}, \tag{1}$$

where the factor α is defined as $\alpha = \frac{n_+}{n_-}$ and n_+, n_- are the total number of H_c^+, H_c^- candidates. This factor accounts for asymmetries arising in the production of H_c^+ baryons, as well as in the detection of the final-state particles. The production and global detection asymmetries do not to depend on the Dalitz plot position.

A numerical comparison between the Dalitz plots of the H_c^+ and H_c^- candidates is made using a χ^2 test defined as

$$\chi^2 \equiv \Sigma (S_{CP}^i)^2. \tag{2}$$

A p-value for the hypothesis of no CPV is obtained from the χ^2 distribution considering that the number of degrees of freedom is equal to the total number of bins minus one, due to the constraint on the factor α of the overall H_c^+ and H_c^- normalisation.

In the hypothesis of no CPV, the S_{CP} values are expected to be distributed according to the normal distribution with a mean of zero and a standard deviation of unity. The test is performed using only bins with a minimum of 10 H_c^+ and 10 H_c^- candidates. In case of CPV, a deviation from the normal distribution is expected, generating a p-value close to zero.

4.2 Unbinned kNN method

The kNN method is based on the concept of a set of nearest neighbour candidates (n_k) in a combined sample of two data sets: baryons and antibaryons. As an unbinned method, the kNN approach is more sensitive to a CPV search in a sample with limited data, compared to that of the binned S_{CP} method. The kNN method is used here to test whether baryons and antibaryons share the same parent distribution function [38–40]. To find the n_k nearest neighbour events of each H_c^+ or H_c^- candidate, an Euclidean distance between closest points in the Dalitz plot is used. A test statistic T for the null hypothesis is defined as

$$T = \frac{1}{n_k(n_+ + n_-)} \sum_{i=1}^{n_+ + n_-} \sum_{k=1}^{n_k} I(i,k), \tag{3}$$

where $I(i,k) = 1$ if the ith candidate and its kth nearest neighbour have the same charge and $I(i,k) = 0$ otherwise.

The test statistic T is the mean fraction of like-charged neighbour pairs in the sample of H_c^+ and H_c^- decays. The advantage of the kNN method, in comparison with other proposed methods for unbinned analyses [38], is that the calculation of T is simple and fast and the expected distribution of T is well known. Under the hypothesis of no CPV, T follows a normal distribution with a mean, μ_T, and a variance, σ_T, where

$$\mu_T = \frac{n_+(n_+ - 1) + n_-(n_- - 1)}{n(n-1)}, \tag{4}$$

$$\lim_{n,n_k,D\to\infty} \sigma_T^2 = \frac{1}{nn_k}\left(\frac{n_+ n_-}{n^2} + 4\frac{n_+^2 n_-^2}{n^4}\right), \tag{5}$$

with $n = n_+ + n_-$ and $D = 2$ is the dimensionality of the tested distribution. A good approximation of σ_T is obtained even for $D = 2$ for the current values of n_+, n_- and n_k [38].

For $n_+ = n_-$ the mean μ_T can be expressed as

$$\mu_{TR} = \frac{1}{2}\left(\frac{n-2}{n-1}\right) \tag{6}$$

and is called the reference value, μ_{TR}. For large n, μ_{TR} asymptotically tends to 0.5.

To increase the power of the kNN method, the Dalitz plot is divided into regions defined around the expected resonances. It can provide one of the necessary conditions for observation of CPV: large relative strong phases in the final states of interfering amplitudes of the intermediate resonance states. The Dalitz plot is partitioned into six regions for the decays of the Λ_c^+ control mode and eleven regions for signal Ξ_c^+ decays according to the present of resonances of the phase space, as shown in Fig. 3. The definitions of the regions are also given in Tables 1 and 2 for Λ_c^+ and Ξ_c^+ baryons, respectively. For Λ_c^+ decays the $K^*(892)$, $K^*(1430)$, $\Delta(1232)$, $\Lambda(1520)$, $\Lambda(1670)$, $\Lambda(1690)$ resonances are seen in data, whilst for Ξ_c^+ decays additional resonances are seen, namely $\Lambda(1520)$, $\Lambda(1600)$, $\Lambda(1710)$, $\Lambda(1800)$, $\Lambda(1810)$, $\Lambda(1820)$, $\Lambda(1830)$, $\Lambda(1890)$, $\Delta(1600)$, $\Delta(1620)$ and $\Delta(1700)$. For Λ_c^+ decays there are four independent regions (R1–R4), whilst the region R2 is further split into the high $M^2(pK^-)$ region (R6) and the

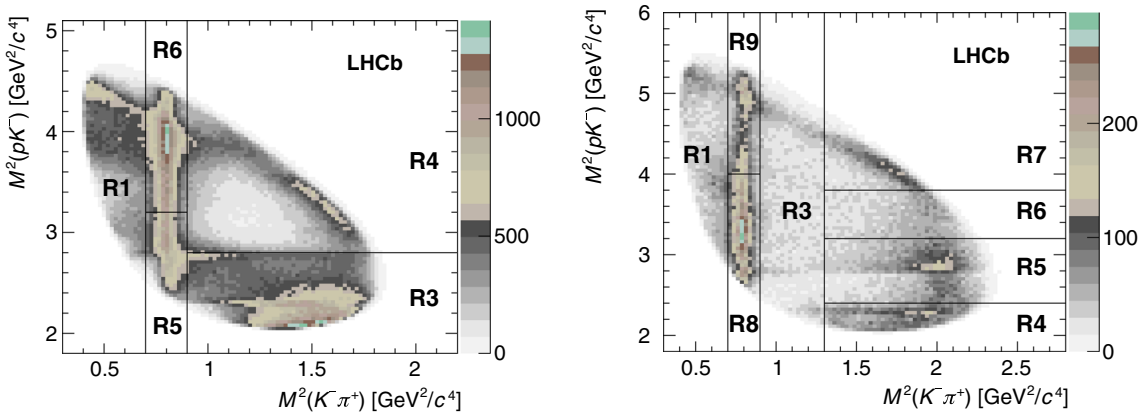

Fig. 3 Definition of the Dalitz plot regions for (left) $\Lambda_c^+ \to pK^-\pi^+$ and (right) $\Xi_c^+ \to pK^-\pi^+$ decays. Additional regions are defined by combining regions. For $\Lambda_c^+ \to pK^-\pi^+$ R2 = R5 ∪ R6 and for $\Xi_c^+ \to pK^-\pi^+$ R2 = R8∪R9, R10 = R4∪R5 and R11 = R4∪R5∪R6∪R7. The presented distributions correspond to the 2012 data sample

Table 1 Definitions of the Dalitz plot regions for the control mode, $\Lambda_c^+ \to pK^-\pi^+$

Region	Definition
R0	Full Dalitz plot
R1	$M^2(K^-\pi^+) < 0.7$ GeV$^2/c^4$
R2	$0.7 \le M^2(K^-\pi^+) < 0.9$ GeV$^2/c^4$
R3	$M^2(K^-\pi^+) \ge 0.9$ GeV$^2/c^4$, $M^2(pK^-) < 2.8$ GeV$^2/c^4$
R4	$M^2(K^-\pi^+) \ge 0.9$ GeV$^2/c^4$, $M^2(pK^-) \ge 2.8$ GeV$^2/c^4$
R5	$0.7 \le M^2(K^-\pi^+) < 0.9$ GeV$^2/c^4$, $M^2(pK^-) < 3.2$ GeV$^2/c^4$
R6	$0.7 \le M^2(K^-\pi^+) < 0.9$ GeV$^2/c^4$, $M^2(pK^-) \ge 3.2$ GeV$^2/c^4$

Table 2 Definitions of the Dalitz plot regions for $\Xi_c^+ \to pK^-\pi^+$ decays

Region	Definition
R0	Full Dalitz plot
R1	$M^2(K^-\pi^+) < 0.7$ GeV$^2/c^4$
R2	$0.7 \le M^2(K^-\pi^+) < 0.9$ GeV$^2/c^4$
R3	$0.9 \le M^2(K^-\pi^+) < 1.3$ GeV$^2/c^4$
R4	$M^2(K^-\pi^+) \ge 1.3$ GeV$^2/c^4$, $M^2(pK^-) < 2.4$ GeV$^2/c^4$
R5	$M^2(K^-\pi^+) \ge 1.3$ GeV$^2/c^4$, $2.4 \le M^2(pK^-) < 3.2$ GeV$^2/c^4$
R6	$M^2(K^-\pi^+) \ge 1.3$ GeV$^2/c^4$, $3.2 \le M^2(pK^-) < 3.8$ GeV$^2/c^4$
R7	$M^2(K^-\pi^+) \ge 1.3$ GeV$^2/c^4$, $M^2(pK^-) \ge 3.8$ GeV$^2/c^4$
R8	$0.7 \le M^2(K^-\pi^+) < 0.9$ GeV$^2/c^4$, $M^2(pK^-) < 4$ GeV$^2/c^4$
R9	$0.7 \le M^2(K^-\pi^+) < 0.9$ GeV$^2/c^4$, $M^2(pK^-) \ge 4$ GeV$^2/c^4$
R10	$M^2(K^-\pi^+) \ge 1.3$ GeV$^2/c^4$, $M^2(pK^-) < 3.2$ GeV$^2/c^4$
R11	$M^2(K^-\pi^+) \ge 1.3$ GeV$^2/c^4$

low $M^2(pK^-)$ region (R5). For Ξ_c^+ there are seven independent regions (R1–R7), whilst the region R2 is split in mass $M^2(pK^-)$ in two regions at larger mass (R9) and smaller mass (R8), R2 = R8∪R9, similarly for R10 and R11, where R10 = R4∪R5, and R11 = R4∪R5∪R6∪R7. Region R0 is the full Dalitz plot.

5 Control mode, background and sensitivity studies

The S_{CP} and kNN methods are tested using the $\Lambda_c^+ \to pK^-\pi^+$ control mode where the *CP* asymmetry is expected to be null [22–30]. The sidebands of $\Xi_c^+ \to pK^-\pi^+$ candidates in the mass regions $2320 < M(pK^-\pi^+) < 2445$ MeV$/c^2$ and $2490 < M(pK^-\pi^+) < 2650$ MeV$/c^2$

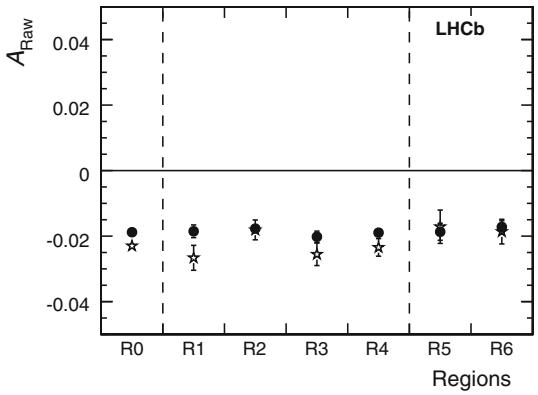

Fig. 4 Measured values of $A_{\rm Raw}$ in regions of $\Lambda_c^+ \to pK^-\pi^+$ candidate decays for 2011 (stars) and 2012 (dots) data samples. R0 corresponds to full Dalitz plot and R2 is separated into R5 and R6, and these regions are correlated and separated by dashed lines

are used to check that the background does not introduce spurious asymmetries.

The measured total raw asymmetry is defined as

$$A_{\rm Raw} = \frac{n_- - n_+}{n_- + n_+}, \tag{7}$$

and it depends on the production asymmetry of H_c^+ baryons and on the detection asymmetries that arise through charge-dependent selection efficiencies due to track reconstruction, trigger selection and particle identification. The measured value of $A_{\rm Raw}$ in each region of the Dalitz plot of $\Lambda_c^+ \to pK^-\pi^+$ decays is presented in Fig. 4. The measured $A_{\rm Raw}$ value integrated over the Dalitz plot equals -0.0230 ± 0.0016 and -0.0188 ± 0.0008 in the 2011 and 2012 data samples, where the uncertainties are statistical only. Within uncertainties, $A_{\rm Raw}$ in all regions amounts to about -2%. There is no significant difference in the measurement of $A_{\rm Raw}$ between the 2011 and 2012 data samples. Since the production and detection asymmetries of Λ_c^+ baryons can depend on the baryon pseudorapidity, η, and $p_{\rm T}$, the dependence of $A_{\rm Raw}$ in regions of the Dalitz plot is checked in bins of η and $p_{\rm T}$ of the Λ_c^+ baryon. It is observed that the value of $A_{\rm Raw}$ globally changes from bin to bin of η and $p_{\rm T}$ of the Λ_c candidates, but for a given bin of η and $p_{\rm T}$ a constant behaviour of $A_{\rm Raw}$ in regions of the Dalitz plot is maintained.

In the S_{CP} method the production asymmetry and all global effects are considered by introducing the α factor, following the strategy described in Sect. 4.1. The p-values obtained are larger than 58%, consistent with the absence of localised asymmetries. As an example, Fig. 5 shows the distribution of S_{CP}^i for $\Lambda_c^+ \to pK^-\pi^+$ decays considering uniform binning, and for two granularities of the Dalitz plot: 28 and 106 bins in the 2012 sample. Alternatively the Dalitz plot is divided into different size bins with the same number of events in each bin. The p-values obtained are larger than

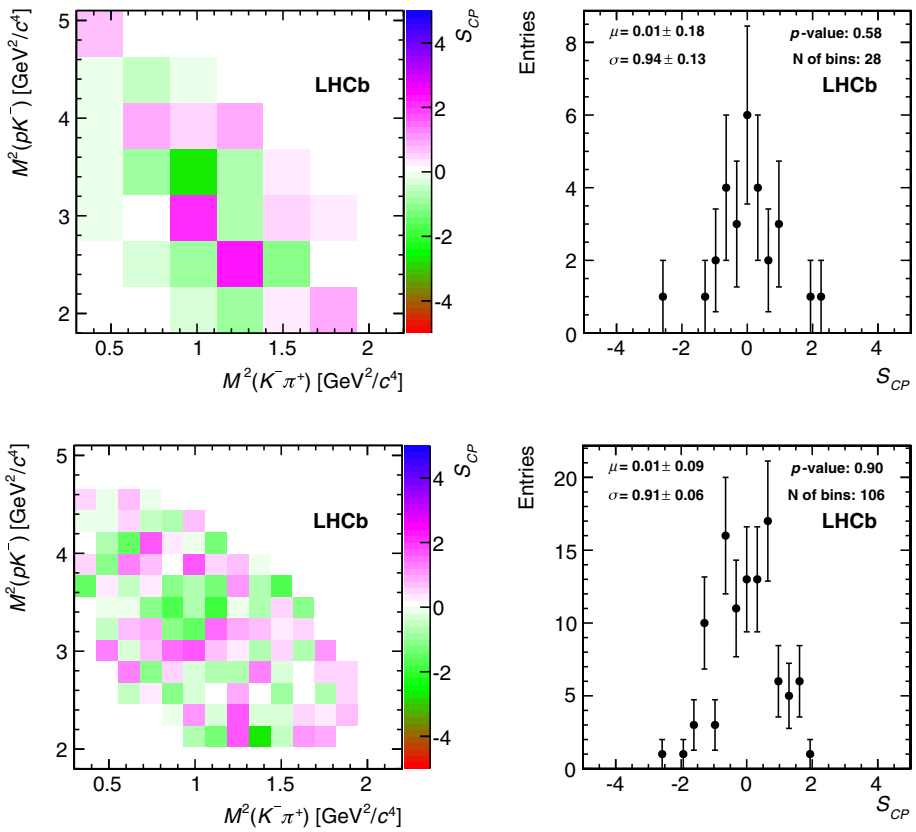

Fig. 5 Distributions of S_{CP}^i and corresponding one-dimensional distributions for $\Lambda_c^+ \to pK^-\pi^+$ decays for the data collected in the 2012 data sample: (top row) 28 same-size bins and (bottom row) 106 same-size bins of the Dalitz plot. The number of analysed bins, nbins, and the p-values are given

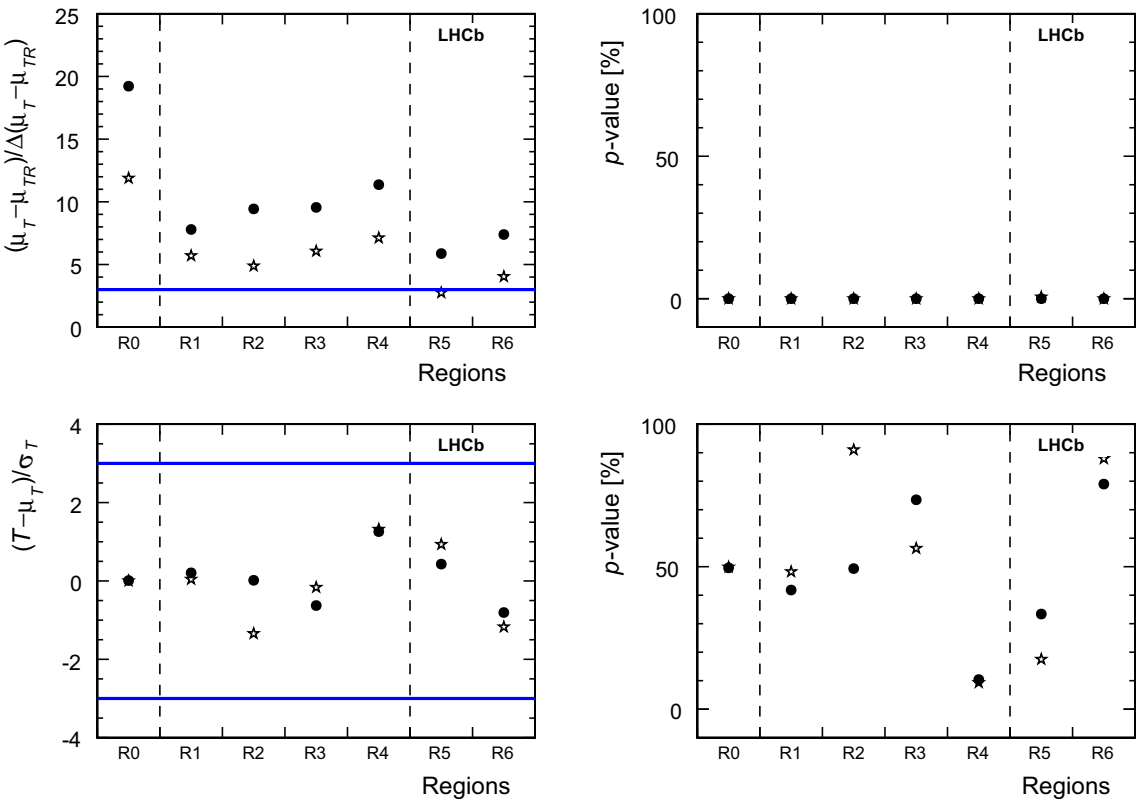

Fig. 6 (Top left) pulls, $(\mu_T - \mu_{TR})/\Delta(\mu_T - \mu_{TR})$, and (top right) the corresponding p-values, (bottom left) pull values of the test statistic T and (bottom right) the corresponding p-values in regions for control $\Lambda_c^+ \to pK^-\pi^+$ candidate decays obtained using the kNN method with $n_k = 50$ for data collected in 2011 (stars) and 2012 (dots). The horizontal lines in the left figures represent -3 and +3 pull values. R0 corresponds to full Dalitz plot and R2 is separated into R5 and R6, and these regions are correlated and separated by dashed lines

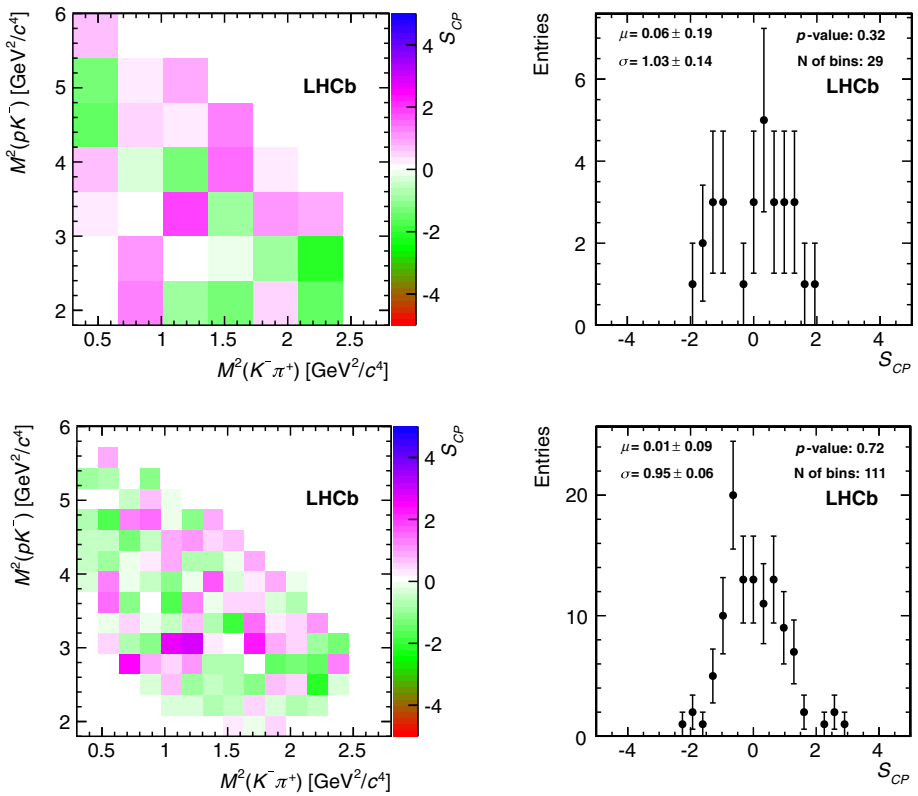

Fig. 7 Distributions of S_{CP}^i and corresponding one-dimensional distributions for $\Xi_c^+ \to pK^-\pi^+$ decays for the combined data collected 2011 and 2012: (top row) 29 uniform bins and (bottom row) 111 uniform bins of the Dalitz plot. The number of analysed bins and the p-values are given

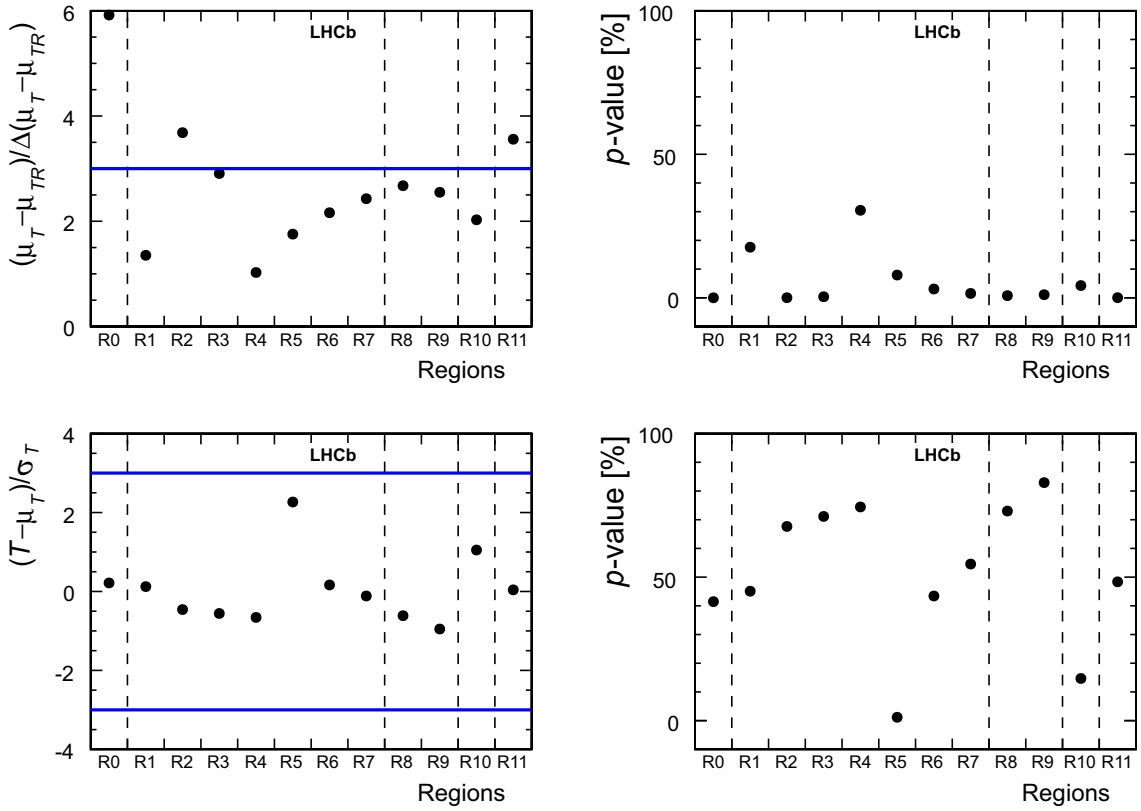

Fig. 8 (Top left) pulls, $(\mu_T - \mu_{TR})/\Delta(\mu_T - \mu_{TR})$, and (top right) the corresponding p-values; (bottom left) pull values of the test statistic T and (bottom right) the corresponding p-values in regions for signal $\Xi_c^+ \to pK^-\pi^+$ candidate decays obtained using the kNN method with $n_k = 50$ for combined data collected 2011 and 2012. The horizontal lines in the left figures represent -3 and $+3$ pull values. R0 corresponds to full Dalitz plot and R2 is separated into R8 and R9, R10 is separated into R4 and R5, R11 is separated into R4, R5, R6 and R7, and these regions are correlated and separated by dashed lines

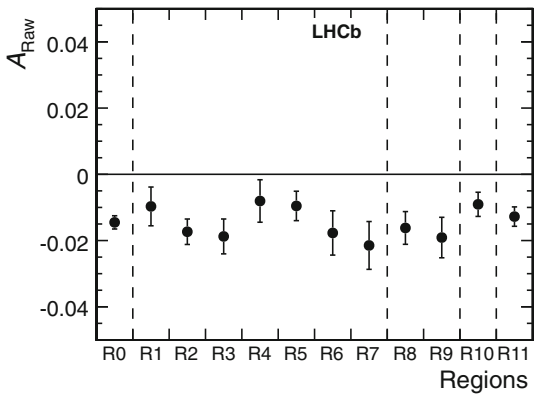

Fig. 9 The measured A_{Raw} in regions in signal $\Xi_c^+ \to pK^-\pi^+$ candidate decays for the combined data collected in 2011 and 2012. R0 corresponds to full Dalitz plot and R2 is separated into R8 and R9, R10 is separated into R4 and R5, R11 is separated into R4, R5, R6 and R7, and these regions are correlated and separated by dashed lines

34%, consistent with the hypothesis of absence of localised asymmetries.

Following the strategy described in Sect. 4.2, the results of the kNN method in regions of the Dalitz plot for the $\Lambda_c^+ \to pK^-\pi^+$ control mode are presented in Fig. 6, for $n_k = 50$. The pulls, $(\mu_T - \mu_{TR})/\Delta(\mu_T - \mu_{TR})$, where $\Delta(\mu_T - \mu_{TR})$ is the statistical uncertainty on the difference $(\mu_T - \mu_{TR})$, are different from zero in all regions. The largest pull value is observed when integrated over the full Dalitz plot. This asymmetry is the result of the nonzero production asymmetry that is presented in Fig. 4 and discussed above. Pulls of the test statistic T, $((T - \mu_T)/\sigma_T)$, vary within -3 and $+3$, consistent with the hypothesis of absence of localised asymmetries in any region. The difference among data-taking years are consistent with statistical fluctuations. Figure 6 illustrates how the larger 2012 data sample improves the power of the kNN method. In Run 2 (years of data taking 2016, 2017 and 2018) the yield is expected to be about three times larger than that from Run 1.

The interaction cross-section of charged hadrons with matter depends on the charged hadron momentum. As such, the detection asymmetries of the proton and kaon-pion systems are momentum dependent. Pseudoexperiments are per-

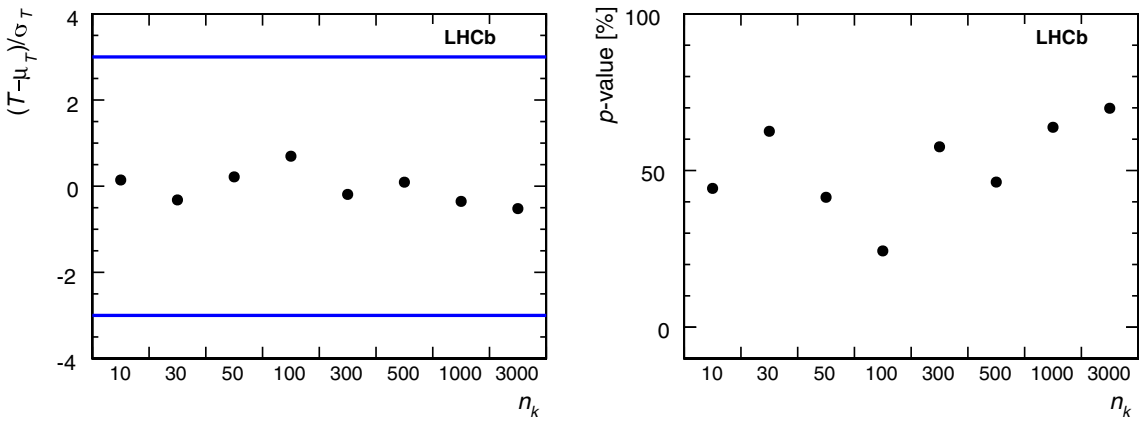

Fig. 10 (Left) the pull values of the test statistic T and (right) the corresponding p-value dependence on the n_k parameter for the whole Dalitz plot (region R0) for $\Xi_c^+ \to pK^-\pi^+$ candidate decays obtained using the kNN method for the combined data collected in 2011 and 2012. The horizontal lines in the left figures represent -3 and $+3$ pull values. The points are determined with different n_k using same data sample, therefore are correlated

formed to check whether the detection asymmetries related to particles reconstructed in the final state can generate a spurious *CP* asymmetry. The proton detection asymmetry varies from about 5% at low momentum to 1% at 100 GeV/c and is estimated using simulations. The kaon-pion detection asymmetry is measured to vary from -1.4% at low momentum to -0.7% at 60 GeV/c [55]. The combined effect of the two asymmetries is found to cancel approximately and does not generate a spurious *CP* asymmetry in the Dalitz plot.

These studies are repeated using the candidates in the sideband of the $\Xi_c^+ \to pK^-\pi^+$ mass distribution. No spurious *CP* asymmetry is found for both methods. For further cross-checks, the control samples are divided according to the polarity of the magnetic field. The p-values are found to be distributed uniformly.

The expected statistical powers of both methods are obtained by performing pseudoexperiments. One hundred samples of $\Xi_c^+ \to pK^-\pi^+$ decays are generated, each with a yield and purity equivalent to that observed in the combined 2011 and 2012 data samples, resulting in 200 000 Ξ_c^+ decays generated in each pseudoexperiment. In this model, the two-dimensional Dalitz plots are generated assuming that the Ξ_c^+ baryons are produced unpolarised. This model is built by including the resonances observed in the data, using the same software as in Ref. [56]. The same resonances as described in Sect. 4.2 are included. The statistical powers of the two methods are found to be comparable. Both methods are sensitive to a 5% *CP* asymmetry in the $K^*(892)$ and $\Delta(1232)$ resonance regions with 3 and 5 sigma significances that would be observed in 69% and 10% of the cases for the kNN method and 17% and 10% of the cases for the S_{CP} method, respectively.

6 Results

6.1 Binned S_{CP} method

The binned S_{CP} method is applied to look for local *CP* asymmetries in $\Xi_c^+ \to pK^-\pi^+$ decays following the strategy described in Sect. 4.1. The distribution of S^i_{CP} for $\Xi_c^+ \to pK^-\pi^+$ decays considering uniform binning, and for two granularities of the Dalitz plot: 29 and 111 bins are shown in Fig. 7 for the combined 2011 and 2012 data samples. The normalization factor α, defined in Eq. 1, is determined to be 1.029 ± 0.004. The measured p-values using a χ^2 test are larger than 32%, consistent with no evidence for *CPV*. The obtained S_{CP} distributions agree with a normal distribution. It is also checked that the results in the 2011 and 2012 data samples are consistent with each other.

6.2 Unbinned kNN method

The unbinned kNN method is applied to look for *CP* asymmetry in $\Xi_c^+ \to pK^-\pi^+$ decays, following the strategy described in Sect. 4.2. The results are presented in Fig. 8 for $n_k = 50$ for the merged 2011 and 2012 data samples. The measured pull values, $((\mu_T - \mu_{TR})/\Delta(\mu_T - \mu_{TR}))$, are different from zero. The largest value of pull is observed integrated over the full Dalitz plot. This is due to the expected nonzero production and detector asymmetries, that is presented in Fig. 9. The measured A_{Raw} is constant within uncertainties in all regions.

The pulls of the test statistic T, $((T - \mu_T)/\sigma_T)$, shown in Fig. 8 vary within -3 and $+3$, consistent with the hypothesis of absence of localised asymmetries. To check for any systematic effects the kNN test is repeated for the individual 2011 and 2012 data samples as well as for samples separated

according to the polarity of the magnetic field. All obtained results are compatible within uncertainties and no systematic effects are observed.

Since the sensitivity of the method can depend on the n_k parameter, the analysis is repeated with different values of n_k from 10 up to 3000. Only T and σ_T depend on n_k. Pulls of the statistic T for the entire Dalitz plot are shown in Fig. 10. All results show no significant deviation from the hypothesis of CP symmetry.

7 Conclusions

Model-independent searches for CP violation in $\Xi_c^+ \to pK^-\pi^+$ decays are presented using the binned S_{CP} and the unbinned kNN methods. The $\Lambda_c^+ \to pK^-\pi^+$ candidates and the sideband regions of $\Xi_c^+ \to pK^-\pi^+$ candidates are used to ensure that no spurious charge asymmetries affect the methods. Both methods are sensitive to CP asymmetry larger than a 5% in the regions around the $K^*(892)$ and the $\Delta(1232)$. The obtained results are consistent with the absence of CP violation in $\Xi_c^+ \to pK^-\pi^+$ decays.

Acknowledgements We express our gratitude to our colleagues in the CERN accelerator departments for the excellent performance of the LHC. We thank the technical and administrative staff at the LHCb institutes. We acknowledge support from CERN and from the national agencies: CAPES, CNPq, FAPERJ and FINEP (Brazil); MOST and NSFC (China); CNRS/IN2P3 (France); BMBF, DFG and MPG (Germany); INFN (Italy); NWO (Netherlands); MNiSW and NCN (Poland); MEN/IFA (Romania); MSHE (Russia); MinECo (Spain); SNSF and SER (Switzerland); NASU (Ukraine); STFC (UK); NSF (USA). We acknowledge the computing resources that are provided by CERN, IN2P3 (France), KIT and DESY (Germany), INFN (Italy), SURF (Netherlands), PIC (Spain), GridPP (UK), RRCKI and Yandex LLC (Russia), CSCS (Switzerland), IFIN-HH (Romania), CBPF (Brazil), PL-GRID (Poland) and OSC (USA). We are indebted to the communities behind the multiple open-source software packages on which we depend. Individual groups or members have received support from AvH Foundation (Germany); EPLANET, Marie Skłodowska-Curie Actions and ERC (European Union); ANR, Labex P2IO and OCEVU, and Région Auvergne-Rhône-Alpes (France); Key Research Program of Frontier Sciences of CAS, CAS PIFI, and the Thousand Talents Program (China); RFBR, RSF and Yandex LLC (Russia); GVA, XuntaGal and GENCAT (Spain); the Royal Society and the Leverhulme Trust (UK); Laboratory Directed Research and Development program of LANL (USA).

Data Availability Statement This manuscript has no associated data or the data will not be deposited. [Authors' comment: The datasets analysed during the current study are available from the corresponding author on reasonable request.]

Funded by SCOAP[3].

References

1. A.D. Sakharov, Violation of CP invariance, C asymmetry, and baryon asymmetry of the universe. Pisma Zh. Eksp. Teor. Fiz. **5**, 32 (1967). https://doi.org/10.1070/PU1991v034n05ABEH002497
2. A.D. Sakharov, Violation of CP invariance, C asymmetry, and baryon asymmetry of the universe. Usp. Fiz. Nauk **161**, 61 (1991)
3. M. Dine, A. Kusenko, The origin of the matter–antimatter asymmetry. Rev. Mod. Phys. **76**, 1 (2003). https://doi.org/10.1103/RevModPhys.76.1. arXiv:hep-ph/0303065
4. N. Cabibbo, Unitary symmetry and leptonic decays. Phys. Rev. Lett. **10**, 531 (1963). https://doi.org/10.1103/PhysRevLett.10.531
5. M. Kobayashi, T. Maskawa, CP-violation in the renormalizable theory of weak interaction. Prog. Theor. Phys. **49**, 652 (1973). https://doi.org/10.1143/PTP.49.652
6. M.B. Gavela, P. Hernandez, J. Orloff, O. Pène, Standard model CP violation and baryon asymmetry. Mod. Phys. Lett. A **9**, 795 (1994). https://doi.org/10.1142/S0217732394000629. arXiv:hep-ph/9312215
7. T. Vieu, A.P. Morais, R. Pasechnik, Electroweak phase transitions in multi-Higgs models: the case of trinification-inspired THDSM. JCAP **1807**, 014 (2018). https://doi.org/10.1088/1475-7516/2018/07/014. arXiv:1801.02670
8. J.H. Christenson, J.W. Cronin, V.L. Fitch, R. Turlay, Evidence for the 2π decay of the K_2^0 meson. Phys. Rev. Lett. **13**, 138 (1964). https://doi.org/10.1103/PhysRevLett.13.138
9. BaBar Collaboration, B. Aubert et al., Observation of CP violation in the B^0 meson system. Phys. Rev. Lett. **87**, 091801 (2001). https://doi.org/10.1103/PhysRevLett.87.091801. arXiv:hep-ex/0107013
10. Belle Collaboration, K. Abe et al., Observation of large CP violation in the neutral B meson system. Phys. Rev. Lett. **87**, 091802 (2001). https://doi.org/10.1103/PhysRevLett.87.091802. arXiv:hep-ex/0107061
11. BaBar Collaboration, B. Aubert et al., Observation of direct CP violation in $B^0 \to K^+\pi^-$ decays. Phys. Rev. Lett. **93**, 131801 (2004). https://doi.org/10.1103/PhysRevLett.93.131801. arXiv:hep-ex/0407057
12. Belle Collaboration, Y. Chao et al., Evidence for direct CP violation in $B^0 \to K^+\pi^-$ decays. Phys. Rev. Lett. **93**, 191802 (2004). https://doi.org/10.1103/PhysRevLett.93.191802. arXiv:hep-ex/0408100
13. LHCb Collaboration, R. Aaij et al., First observation of CP violation in the decays of B_s^0 mesons. Phys. Rev. Lett. **110**, 221601 (2013). https://doi.org/10.1103/PhysRevLett.110.221601. arXiv:1304.6173
14. LHCb Collaboration, R. Aaij et al., Observation of CP violation in $B^\pm \to DK^\pm$ decays. Phys. Lett. B **712**, 203 (2012). https://doi.org/10.1016/j.physletb.2012.04.060. arXiv:1203.3662 [Erratum Phys. Lett. B **713**, 351 (2012). https://doi.org/10.1016/j.physletb.2012.05.060]
15. LHCb Collaboration, R. Aaij et al., Observation of CP violation in charm decays. Phys. Rev. Lett. **122**, 211803 (2019). https://doi.org/10.1103/PhysRevLett.117.211803. arXiv:1903.08726
16. LHCb Collaboration, R. Aaij et al., Search for CP violation in $\Lambda_c \to pK^-K^+$ and $\Lambda_c \to p\pi^-\pi^+$ decays. JHEP **03**, 182 (2018). https://doi.org/10.1007/JHEP03(2018)182. arXiv:1712.07051

17. LHCb Collaboration, R. Aaij et al., Measurement of matter–antimatter differences in beauty baryon decays. Nat. Phys. **13**, 391 (2017). https://doi.org/10.1038/nphys4021. arXiv:1609.05216
18. LHCb Collaboration, R. Aaij et al., Search for CP violation in $\Lambda_b^0 \to p\pi^-\pi^+\pi^-$ decays. arXiv:1912.10741
19. C. Zemach, Three pion decays of unstable particles. Phys. Rev. **133**, B1201 (1964). https://doi.org/10.1103/PhysRev.133.B1201
20. LHCb Collaboration, R. Aaij et al., Observation of several sources of CP violation in $B^+ \to \pi^+\pi^+\pi^-$ decays. Phys. Rev. Lett. **124**, 031801 (2020). https://doi.org/10.1103/PhysRevLett.124.031801. arXiv:1909.05211
21. S. Bianco, F.L. Fabbri, D. Benson, I. Bigi, A Cicerone for the physics of charm. Riv. Nuovo Cim. **26N7**, 1 (2003). https://doi.org/10.1393/ncr/i2003-10003-1. arXiv:hep-ex/0309021
22. I. Shipsey, Status of charm flavor physics. Int. J. Mod. Phys. A **21**, 5381 (2006). https://doi.org/10.1142/S0217751X06034525. arXiv:hep-ex/0607070
23. M. Artuso, B. Meadows, A. Petrov, Charm meson decays. Ann. Rev. Nucl. Part. Sci **58**, 249 (2008). https://doi.org/10.1146/annurev.nucl.58.110707.171131
24. S. Bianco, I.I. Bigi, 2019 Lessons from $\tau(\Omega_c^0)$ and CP asymmetry in charm decays. arXiv:2001.06908
25. Y. Grossman, S. Schacht, The emergence of the $\Delta U = 0$ rule in charm physics. JHEP **07**, 020 (2019). https://doi.org/10.1007/JHEP07(2019)020. arXiv:1903.10952
26. H.-N. Li, C.-D. Lü, F.-S. Yu, Implications on the first observation of charm CPV at LHCb. arXiv:1903.10638
27. H.-Y. Cheng, C.-W. Chiang, Revisiting CP violation in $D \to PP$ and VP decays. Phys. Rev. D **100**, 093002 (2019). https://doi.org/10.1103/PhysRevD.100.093002. arXiv:1909.03063
28. L. Calibbi, T. Li, Y. Li, B. Zhu, Simple model for large CP violation in charm decays, B-physics anomalies, muon g-2, and dark matter. arXiv:1912.02676
29. M. Chala, A. Lenz, A.V. Rusov, J. Scholtz, ΔA_{CP} within the standard model and beyond. JHEP **07**, 161 (2019). https://doi.org/10.1007/JHEP07(2019)161. arXiv:1903.10490
30. A. Dery, Y. Nir, Implications of the LHCb discovery of CP violation in charm decays. JHEP **12**, 104 (2019). https://doi.org/10.1007/JHEP12(2019)104. arXiv:1909.11242
31. Y. Grossman, A.L. Kagan, Y. Nir, New physics and CP violation in singly Cabibbo suppressed D decays. Phys. Rev. D **75**, 036008 (2007). https://doi.org/10.1103/PhysRevD.75.036008. arXiv:hep-ph/0609178
32. I.I. Bigi, Probing CP asymmetries in charm baryons decays. arXiv:1206.4554
33. Y. Grossman, S. Schacht, U-spin sum rules for CP asymmetries of three-body charmed baryon decays. Phys. Rev. D **99**, 033005 (2019). https://doi.org/10.1103/PhysRevD.99.033005. arXiv:1811.11188
34. X.-D. Shi et al., Prospects for CP and P violation in Λ_c^+ decays at super tau charm facility. Phys. Rev. D **100**, 113002 (2019). https://doi.org/10.1103/PhysRevD.100.113002. arXiv:1904.12415
35. D. Wang, Sum rules for CP asymmetries of charmed baryon decays in the $SU(3)_F$ limit. Eur. Phys. J. C **79**, 429 (2019). https://doi.org/10.1140/epjc/s10052-019-6925-y. arXiv:1901.01776
36. LHCb Collaboration, R. Aaij et al., Measurement of the $\Lambda_b^0 \to J/\psi\Lambda$ angular distribution and the Λ_b^0 polarisation in pp collisions. JHEP. arXiv:2004.10563 (submitted)
37. I. Bediaga et al., On a CP anisotropy measurement in the Dalitz plot. Phys. Rev. D **80**, 096006 (2009). https://doi.org/10.1103/PhysRevD.80.096006. arXiv:0905.4233
38. M. Williams, How good are your fits? Unbinned multivariate goodness-of-fit tests in high energy physics. JINST **5**, P09004 (2010). https://doi.org/10.1088/1748-0221/5/09/P09004. arXiv:1006.3019
39. N. Henze, A multivariate two-sample test based on the number of nearest neighbor type coincidences. Ann. Stat. **16**(2), 772 (1988)
40. M.F. Schilling, Multivariate two-sample tests based on nearest neighbors. J. Am. Stat. Assoc. **81**, 799 (1986)
41. LHCb Collaboration, R. Aaij et al., Search for CP violation in the decay $D^+ \to \pi^-\pi^+\pi^+$. Phys. Lett. B **728**, 585 (2014). https://doi.org/10.1016/j.physletb.2013.12.035. arXiv:1310.7953
42. LHCb Collaboration, A.A. Alves Jr. et al., The LHCb detector at the LHC. JINST **3**, S08005 (2008). https://doi.org/10.1088/1748-0221/3/08/S08005
43. LHCb Collaboration, R. Aaij et al., LHCb detector performance. Int. J. Mod. Phys. A **30**, 1530022 (2015). https://doi.org/10.1142/S0217751X15300227. arXiv:1412.6352
44. T. Sjöstrand, S. Mrenna, P. Skands, A brief introduction to PYTHIA 8.1. Comput. Phys. Commun. **178**, 852 (2008). https://doi.org/10.1016/j.cpc.2008.01.036. arXiv:0710.3820
45. I. Belyaev et al., Handling of the generation of primary events in Gauss, the LHCb simulation framework. J. Phys. Conf. Ser. **331**, 032047 (2011). https://doi.org/10.1088/1742-6596/331/3/032047
46. D.J. Lange, The EvtGen particle decay simulation package. Nucl. Instrum. Methods **A462**, 152 (2001). https://doi.org/10.1016/S0168-9002(01)00089-4
47. P. Golonka, Z. Was, PHOTOS Monte Carlo: a precision tool for QED corrections in Z and W decays. Eur. Phys. J. C **45**, 97 (2006). https://doi.org/10.1140/epjc/s2005-02396-4. arXiv:hep-ph/0506026
48. Geant4 Collaboration, J. Allison et al., Geant4 developments and applications. IEEE Trans. Nucl. Sci. **53**, 270 (2006). https://doi.org/10.1109/TNS.2006.869826
49. M. Clemencic et al., The LHCb simulation application, Gauss: design, evolution and experience. J. Phys. Conf. Ser. **331**, 032023 (2011). https://doi.org/10.1088/1742-6596/331/3/032023
50. Particle Data Group, M. Tanabashi et al., Review of particle physics. Phys. Rev. D **98**, 030001 (2018). https://doi.org/10.1103/PhysRevD.98.030001
51. BaBar Collaboration, B. Aubert et al., A search for CP violation and a measurement of the relative branching fraction in $D^+ \to K^-K^+\pi^+$ decays. Phys. Rev. D **71**, 091101 (2005). https://doi.org/10.1103/PhysRevD.71.091101. arXiv:hep-ex/0501075
52. BaBar Collaboration, B. Aubert et al., Search for CP violation in neutral D meson Cabibbo-suppressed three-body decays. Phys. Rev. D **78**, 051102 (2008). https://doi.org/10.1103/PhysRevD.78.051102. arXiv:0802.4035
53. LHCb Collaboration, R. Aaij et al., Search for CP violation in $D^+ \to K^-K^+\pi^+$ decays. Phys. Rev. D **84**, 112008 (2011). https://doi.org/10.1103/PhysRevD.84.112008. arXiv:1110.3970
54. LHCb Collaboration, R. Aaij et al., Observation of the $\Lambda_b^0 \to J/\psi p\pi^-$ decay. JHEP **07**, 103 (2014). https://doi.org/10.1007/JHEP07(2014)103. arXiv:1406.0755
55. LHCb Collaboration, R. Aaij et al., Measurement of CP asymmetry in $D^0 \to K^-K^+$ and $D^0 \to \pi^-\pi^+$ decays. JHEP **07**, 041 (2014). https://doi.org/10.1007/JHEP07(2014)041. arXiv:1405.2797
56. LHCb Collaboration, R. Aaij et al., Study of the D^0p amplitude in $\Lambda_b^0 \to D^0p\pi^-$ decays. JHEP **05**, 030 (2017). https://doi.org/10.1007/JHEP05(2017)030. arXiv:1701.07873

LHCb Collaboration

R. Aaij[31], C. Abellán Beteta[49], T. Ackernley[59], B. Adeva[45], M. Adinolfi[53], H. Afsharnia[9], C. A. Aidala[79], S. Aiola[25], Z. Ajaltouni[9], S. Akar[64], P. Albicocco[22], J. Albrecht[14], F. Alessio[47], M. Alexander[58], A. Alfonso Albero[44], G. Alkhazov[37], P. Alvarez Cartelle[60], A. A. Alves Jr[45], S. Amato[2], Y. Amhis[11], L. An[21], L. Anderlini[21], G. Andreassi[48], M. Andreotti[20], F. Archilli[16], J. Arnau Romeu[10], A. Artamonov[43], M. Artuso[67], K. Arzymatov[41], E. Aslanides[10], M. Atzeni[49], B. Audurier[26], S. Bachmann[16], J. J. Back[55], S. Baker[60], V. Balagura[11,b], W. Baldini[20,47], A. Baranov[41], R. J. Barlow[61], S. Barsuk[11], W. Barter[60], M. Bartolini[23,h], F. Baryshnikov[76], J. M. Basels[13], G. Bassi[28], V. Batozskaya[35], B. Batsukh[67], A. Battig[14], V. Battista[48], A. Bay[48], M. Becker[14], F. Bedeschi[28], I. Bediaga[1], A. Beiter[67], L. J. Bel[31], V. Belavin[41], S. Belin[26], N. Beliy[5], V. Bellee[48], K. Belous[43], I. Belyaev[38], G. Bencivenni[22], E. Ben-Haim[12], S. Benson[31], S. Beranek[13], A. Berezhnoy[39], R. Bernet[49], D. Berninghoff[16], H. C. Bernstein[67], C. Bertella[47], E. Bertholet[12], A. Bertolin[27], C. Betancourt[49], F. Betti[19,e], M. O. Bettler[54], Ia. Bezshyiko[49], S. Bhasin[53], J. Bhom[33], M. S. Bieker[14], S. Bifani[52], P. Billoir[12], A. Birnkraut[14], A. Bizzeti[21,u], M. Bjørn[62], M. P. Blago[47], T. Blake[55], F. Blanc[48], S. Blusk[67], D. Bobulska[58], V. Bocci[30], O. Boente Garcia[45], T. Boettcher[63], A. Boldyrev[77], A. Bondar[42,x], N. Bondar[37], S. Borghi[47,61], M. Borisyak[41], M. Borsato[16], J. T. Borsuk[33], M. Boubdir[13], T. J. V. Bowcock[59], C. Bozzi[20,47], M. J. Bradley[60], S. Braun[16], A. Brea Rodriguez[45], M. Brodski[47], J. Brodzicka[33], A. Brossa Gonzalo[55], D. Brundu[26,47], E. Buchanan[53], A. Büchler-Germann[49], A. Buonaura[49], C. Burr[47], A. Bursche[26], A. Butkevich[40], J. S. Butter[31], J. Buytaert[47], W. Byczynski[47], S. Cadeddu[26], H. Cai[71], R. Calabrese[20,g], L. Calero Diaz[22], S. Cali[22], R. Calladine[52], M. Calvi[24,i], M. Calvo Gomez[44,m], P. Camargo Magalhaes[53], A. Camboni[44,m], P. Campana[22], D. H. Campora Perez[47], A. F. Campoverde Quezada[5], L. Capriotti[19,e], A. Carbone[19,e], G. Carboni[29], R. Cardinale[23,h], A. Cardini[26], I. Carli[6], P. Carniti[24,i], K. Carvalho Akiba[31], A. Casais Vidal[45], G. Casse[59], M. Cattaneo[47], G. Cavallero[23], S. Celani[48], R. Cenci[28,p], J. Cerasoli[10], M. G. Chapman[53], M. Charles[12,47], Ph. Charpentier[47], G. Chatzikonstantinidis[52], M. Chefdeville[8], V. Chekalina[41], C. Chen[3], S. Chen[26], A. Chernov[33], S.-G. Chitic[47], V. Chobanova[45], S. Cholak[48], M. Chrzaszcz[47], A. Chubykin[37], P. Ciambrone[22], M. F. Cicala[55], X. Cid Vidal[45], G. Ciezarek[47], F. Cindolo[19], P. E. L. Clarke[57], M. Clemencic[47], H. V. Cliff[54], J. Closier[47], J. L. Cobbledick[61], V. Coco[47], J. A. B. Coelho[11], J. Cogan[10], E. Cogneras[9], L. Cojocariu[36], P. Collins[47], T. Colombo[47], A. Comerma-Montells[16], A. Contu[26], N. Cooke[52], G. Coombs[58], S. Coquereau[44], G. Corti[47], C. M. Costa Sobral[55], B. Couturier[47], G. A. Cowan[57], D. C. Craik[63], J. Crkovská[66], A. Crocombe[55], M. Cruz Torres[1], R. Currie[57], C. L. Da Silva[66], E. Dall'Occo[31], J. Dalseno[45,53], C. D'Ambrosio[47], A. Danilina[38], P. d'Argent[16], A. Davis[61], O. De Aguiar Francisco[47], K. De Bruyn[47], S. De Capua[61], M. De Cian[48], J. M. De Miranda[1], L. De Paula[2], M. De Serio[18,d], P. De Simone[22], J. A. de Vries[31], C. T. Dean[66], W. Dean[79], D. Decamp[8], L. Del Buono[12], B. Delaney[54], H.-P. Dembinski[15], M. Demmer[14], A. Dendek[34], V. Denysenko[49], D. Derkach[77], O. Deschamps[9], F. Desse[11], F. Dettori[26,f], B. Dey[7], A. Di Canto[47], P. Di Nezza[22], S. Didenko[76], H. Dijkstra[47], V. Dobishuk[51], F. Dordei[26], M. Dorigo[28,y], A. C. dos Reis[1], A. Dosil Suárez[45], L. Douglas[58], A. Dovbnya[50], K. Dreimanis[59], M. W. Dudek[33], G. Dujany[12], P. Durante[47], J. M. Durham[66], D. Dutta[61], R. Dzhelyadin[43,†], M. Dziewiecki[16], A. Dziurda[33], A. Dzyuba[37], S. Easo[56], U. Egede[60], V. Egorychev[38], S. Eidelman[42,x], S. Eisenhardt[57], R. Ekelhof[14], S. Ek-In[48], L. Eklund[58], S. Ely[67], A. Ene[36], E. Epple[66], S. Escher[13], S. Esen[31], T. Evans[47], A. Falabella[19], J. Fan[3], Y. Fan[5], N. Farley[52], S. Farry[59], D. Fazzini[11], P. Fedin[38], M. Féo[47], P. Fernandez Declara[47], A. Fernandez Prieto[45], F. Ferrari[19,e], L. Ferreira Lopes[48], F. Ferreira Rodrigues[2], S. Ferreres Sole[31], M. Ferrillo[49], M. Ferro-Luzzi[47], S. Filippov[40], R. A. Fini[18], M. Fiorini[20,g], M. Firlej[34], K. M. Fischer[62], C. Fitzpatrick[47], T. Fiutowski[34], F. Fleuret[11,b], M. Fontana[47], F. Fontanelli[23,h], R. Forty[47], V. Franco Lima[59], M. Franco Sevilla[65], M. Frank[47], C. Frei[47], D. A. Friday[58], J. Fu[25,q], Q. Fuehring[14], W. Funk[47], E. Gabriel[57], A. Gallas Torreira[45], D. Galli[19,e], S. Gallorini[27], S. Gambetta[57], Y. Gan[3], M. Gandelman[2], P. Gandini[25], Y. Gao[4], L. M. Garcia Martin[46], J. García Pardiñas[49], B. Garcia Plana[45], F. A. Garcia Rosales[11], J. Garra Tico[54], L. Garrido[44], D. Gascon[44], C. Gaspar[47], G. Gazzoni[9], D. Gerick[16], E. Gersabeck[61], M. Gersabeck[61], T. Gershon[55], D. Gerstel[10], Ph. Ghez[8], V. Gibson[54], A. Gioventù[45], O. G. Girard[48], P. Gironella Gironell[44], L. Giubega[36], C. Giugliano[20,g], K. Gizdov[57], V. V. Gligorov[12], C. Göbel[69], E. Golobardes[44,m], D. Golubkov[38], A. Golutvin[60,76], A. Gomes[1,a], P. Gorbounov[38,47], I. V. Gorelov[39], C. Gotti[24,i], E. Govorkova[31], J. P. Grabowski[16], R. Graciani Diaz[44], T. Grammatico[12], L. A. Granado Cardoso[47], E. Graugés[44], E. Graverini[48], G. Graziani[21], A. Grecu[36], R. Greim[31], P. Griffith[20,g], L. Grillo[61], L. Gruber[47], B. R. Gruberg Cazon[62], C. Gu[3], P. A. Günther[16], X. Guo[70], E. Gushchin[40], A. Guth[13], Yu. Guz[43,47], T. Gys[47], T. Hadavizadeh[62], C. Hadjivasiliou[9], G. Haefeli[48], C. Haen[47], S. C. Haines[54], P. M. Hamilton[65], Q. Han[7], X. Han[16], T. H. Hancock[62], S. Hansmann-Menzemer[16], N. Harnew[62], T. Harrison[59], R. Hart[31], C. Hasse[47], M. Hatch[47], J. He[5], M. Hecker[60], K. Heijhoff[31], K. Heinicke[14], A. Heister[14], A. M. Hennequin[47], K. Hennessy[59], L. Henry[46], M. Heß[73], J. Heuel[13], A. Hicheur[68], R. Hidalgo Charman[61], D. Hill[62], M. Hilton[61], P. H. Hopchev[48], J. Hu[16], W. Hu[7], W. Huang[5], Z. C. Huard[64], W. Hulsbergen[31], T. Humair[60],

R. J. Hunter[55], M. Hushchyn[77], D. Hutchcroft[59], D. Hynds[31], P. Ibis[14], M. Idzik[34], P. Ilten[52], A. Inglessi[37], A. Inyakin[43], K. Ivshin[37], R. Jacobsson[47], S. Jakobsen[47], J. Jalocha[62], E. Jans[31], B. K. Jashal[46], A. Jawahery[65], V. Jevtic[14], F. Jiang[3], M. John[62], D. Johnson[47], C. R. Jones[54], B. Jost[47], N. Jurik[62], S. Kandybei[50], M. Karacson[47], J. M. Kariuki[53], S. Karodia[58], N. Kazeev[77], M. Kecke[16], F. Keizer[54], M. Kelsey[67], M. Kenzie[54], T. Ketel[32], B. Khanji[47], A. Kharisova[78], C. Khurewathanakul[48], K. E. Kim[67], T. Kirn[13], V. S. Kirsebom[48], S. Klaver[22], K. Klimaszewski[35], S. Koliiev[51], A. Kondybayeva[76], A. Konoplyannikov[38], P. Kopciewicz[34], R. Kopecna[16], P. Koppenburg[31], M. Korolev[39], I. Kostiuk[31,51], O. Kot[51], S. Kotriakhova[37], M. Kozeiha[9], L. Kravchuk[40], R. D. Krawczyk[47], M. Kreps[55], F. Kress[60], S. Kretzschmar[13], P. Krokovny[42,x], W. Krupa[34], W. Krzemien[35], W. Kucewicz[33,l], M. Kucharczyk[33], V. Kudryavtsev[42,x], H. S. Kuindersma[31], G. J. Kunde[66], A. K. Kuonen[48], T. Kvaratskheliya[38], D. Lacarrere[47], G. Lafferty[61], A. Lai[26], D. Lancierini[49], J. J. Lane[61], G. Lanfranchi[22], C. Langenbruch[13], O. Lantwin[49], T. Latham[55], F. Lazzari[28,v], C. Lazzeroni[52], R. Le Gac[10], R. Lefèvre[9], A. Leflat[39], F. Lemaitre[47], O. Leroy[10], T. Lesiak[33], B. Leverington[16], H. Li[70], L. Li[62], P.-R. Li[5], X. Li[66], Y. Li[6], Z. Li[67], X. Liang[67], R. Lindner[47], P. Ling[70], F. Lionetto[49], V. Lisovskyi[11], G. Liu[70], X. Liu[3], D. Loh[55], A. Loi[26], J. Lomba Castro[45], I. Longstaff[58], J. H. Lopes[2], G. Loustau[49], G. H. Lovell[54], Y. Lu[6], D. Lucchesi[27,o], M. Lucio Martinez[31], Y. Luo[3], A. Lupato[27], E. Luppi[20,g], O. Lupton[55], A. Lusiani[28,t], X. Lyu[5], R. Ma[70], S. Maccolini[19,e], F. Machefert[11], F. Maciuc[36], V. Macko[48], P. Mackowiak[14], S. Maddrell-Mander[53], L. R. Madhan Mohan[53], O. Maev[37,47], A. Maevskiy[77], K. Maguire[61], D. Maisuzenko[37], M. W. Majewski[34], S. Malde[62], B. Malecki[47], A. Malinin[75], T. Maltsev[42,x], H. Malygina[16], G. Manca[26,f], G. Mancinelli[10], R. Manera Escalero[44], D. Manuzzi[19,e], D. Marangotto[25,q], J. Maratas[9,w], J. F. Marchand[8], U. Marconi[19], S. Mariani[21], C. Marin Benito[11], M. Marinangeli[48], P. Marino[48], J. Marks[16], P. J. Marshall[59], G. Martellotti[30], L. Martinazzoli[47], M. Martinelli[24,47,i], D. Martinez Santos[45], F. Martinez Vidal[46], A. Massafferri[1], M. Materok[13], R. Matev[47], A. Mathad[49], Z. Mathe[47], V. Matiunin[38], C. Matteuzzi[24], K. R. Mattioli[79], A. Mauri[49], E. Maurice[11,b], M. McCann[47,60], L. Mcconnell[17], A. McNab[61], R. McNulty[17], J. V. Mead[59], B. Meadows[64], C. Meaux[10], G. Meier[14], N. Meinert[73], D. Melnychuk[35], S. Meloni[24,i], M. Merk[31], A. Merli[25], E. Michielin[27], M. Mikhasenko[47], D. A. Milanes[72], E. Millard[55], M.-N. Minard[8], O. Mineev[38], L. Minzoni[20,g], S. E. Mitchell[57], B. Mitreska[61], D. S. Mitzel[47], A. Mödden[14], A. Mogini[12], R. D. Moise[60], T. Mombächer[14], I. A. Monroy[72], S. Monteil[9], M. Morandin[27], G. Morello[22], M. J. Morello[28,t], J. Moron[34], A. B. Morris[10], A. G. Morris[55], R. Mountain[67], H. Mu[3], F. Muheim[57], M. Mukherjee[7], M. Mulder[31], D. Müller[47], J. Müller[14], K. Müller[49], V. Müller[14], C. H. Murphy[62], D. Murray[61], P. Muzzetto[26], P. Naik[53], T. Nakada[48], R. Nandakumar[56], A. Nandi[62], T. Nanut[48], I. Nasteva[2], M. Needham[57], N. Neri[25,q], S. Neubert[16], N. Neufeld[47], R. Newcombe[60], T. D. Nguyen[48], C. Nguyen-Mau[48,n], E. M. Niel[11], S. Nieswand[13], N. Nikitin[39], N. S. Nolte[47], C. Nunez[79], A. Oblakowska-Mucha[34], V. Obraztsov[43], S. Ogilvy[58], D. P. O'Hanlon[19], R. Oldeman[26,f], C. J. G. Onderwater[74], J. D. Osborn[79], A. Ossowska[33], J. M. Otalora Goicochea[2], T. Ovsiannikova[38], P. Owen[49], A. Oyanguren[46], P. R. Pais[48], T. Pajero[28,t], A. Palano[18], M. Palutan[22], G. Panshin[78], A. Papanestis[56], M. Pappagallo[57], L. L. Pappalardo[20,g], W. Parker[65], C. Parkes[47,61], G. Passaleva[21,47], A. Pastore[18], M. Patel[60], C. Patrignani[19,e], A. Pearce[47], A. Pellegrino[31], G. Penso[30], M. Pepe Altarelli[47], S. Perazzini[19], D. Pereima[38], P. Perret[9], L. Pescatore[48], K. Petridis[53], A. Petrolini[23,h], A. Petrov[75], S. Petrucci[57], M. Petruzzo[25,q], B. Pietrzyk[8], G. Pietrzyk[48], M. Pikies[33], M. Pili[62], D. Pinci[30], J. Pinzino[47], F. Pisani[47], A. Piucci[16], V. Placinta[36], S. Playfer[57], J. Plews[52], M. Plo Casasus[45], F. Polci[12], M. Poli Lener[22], M. Poliakova[67], A. Poluektov[10], N. Polukhina[76,c], I. Polyakov[67], E. Polycarpo[2], G. J. Pomery[53], S. Ponce[47], A. Popov[43], D. Popov[52], S. Poslavskii[43], K. Prasanth[33], L. Promberger[47], C. Prouve[45], V. Pugatch[51], A. Puig Navarro[49], H. Pullen[62], G. Punzi[28,p], W. Qian[5], J. Qin[5], R. Quagliani[12], B. Quintana[9], N. V. Raab[17], R. I. Rabadan Trejo[10], B. Rachwal[34], J. H. Rademacker[53], M. Rama[28], M. Ramos Pernas[45], M. S. Rangel[2], F. Ratnikov[41,77], G. Raven[32], M. Ravonel Salzgeber[47], M. Reboud[8], F. Redi[48], S. Reichert[14], F. Reiss[12], C. Remon Alepuz[46], Z. Ren[3], V. Renaudin[62], S. Ricciardi[56], D. S. Richards[56], S. Richards[53], K. Rinnert[59], P. Robbe[11], A. Robert[12], A. B. Rodrigues[48], E. Rodrigues[64], J. A. Rodriguez Lopez[72], M. Roehrken[47], S. Roiser[47], A. Rollings[62], V. Romanovskiy[43], M. Romero Lamas[45], A. Romero Vidal[45], J. D. Roth[79], M. Rotondo[22], M. S. Rudolph[67], T. Ruf[47], J. Ruiz Vidal[46], A. Ryzhikov[77], J. Ryzka[34], J. J. Saborido Silva[45], N. Sagidova[37], N. Sahoo[55], B. Saitta[26,f], C. Sanchez Gras[31], C. Sanchez Mayordomo[46], B. Sanmartin Sedes[45], R. Santacesaria[30], C. Santamarina Rios[45], M. Santimaria[22,47], E. Santovetti[29,j], G. Sarpis[61], A. Sarti[30], C. Satriano[30,s], A. Satta[29], M. Saur[5], D. Savrina[38,39], L. G. Scantlebury Smead[62], S. Schael[13], M. Schellenberg[14], M. Schiller[58], H. Schindler[47], M. Schmelling[15], T. Schmelzer[14], B. Schmidt[47], O. Schneider[48], A. Schopper[47], H. F. Schreiner[64], M. Schubiger[31], S. Schulte[48], M. H. Schune[11], R. Schwemmer[47], B. Sciascia[22], A. Sciubba[30,k], S. Sellam[68], A. Semennikov[38], A. Sergi[47,52], N. Serra[49], J. Serrano[10], L. Sestini[27], A. Seuthe[14], P. Seyfert[47], D. M. Shangase[79], M. Shapkin[43], L. Shchutska[48], T. Shears[59], L. Shekhtman[42,x], V. Shevchenko[75,76], E. Shmanin[76], J. D. Shupperd[67], B. G. Siddi[20], R. Silva Coutinho[49], L. Silva de Oliveira[2], G. Simi[27,o], S. Simone[18,d], I. Skiba[20,g], N. Skidmore[16], T. Skwarnicki[67], M. W. Slater[52], J. G. Smeaton[54], A. Smetkina[38], E. Smith[13], I. T. Smith[57], M. Smith[60], A. Snoch[31], M. Soares[19], L. Soares Lavra[1], M. D. Sokoloff[64], F. J. P. Soler[58], B. Souza De Paula[2], B. Spaan[14], E. Spadaro Norella[25,q], P. Spradlin[58],

F. Stagni[47], M. Stahl[64], S. Stahl[47], P. Stefko[48], S. Stefkova[60], O. Steinkamp[49], S. Stemmle[16], O. Stenyakin[43], M. Stepanova[37], H. Stevens[14], S. Stone[67], S. Stracka[28], M. E. Stramaglia[48], M. Straticiuc[36], U. Straumann[49], S. Strokov[78], J. Sun[3], L. Sun[71], Y. Sun[65], P. Svihra[61], K. Swientek[34], A. Szabelski[35], T. Szumlak[34], M. Szymanski[5], S. Taneja[61], Z. Tang[3], T. Tekampe[14], G. Tellarini[20], F. Teubert[47], E. Thomas[47], K. A. Thomson[59], M. J. Tilley[60], V. Tisserand[9], S. T'Jampens[8], M. Tobin[6], S. Tolk[47], L. Tomassetti[20,g], D. Tonelli[28], D. Torres Machado[1], D. Y. Tou[12], E. Tournefier[8], M. Traill[58], M. T. Tran[48], E. Trifonova[76], C. Trippl[48], A. Trisovic[54], A. Tsaregorodtsev[10], G. Tuci[28,47,p], A. Tully[54], N. Tuning[31], A. Ukleja[35], A. Usachov[11], A. Ustyuzhanin[41,77], U. Uwer[16], A. Vagner[78], V. Vagnoni[19], A. Valassi[47], S. Valat[47], G. Valenti[19], M. van Beuzekom[31], H. Van Hecke[66], E. van Herwijnen[47], C. B. Van Hulse[17], J. van Tilburg[31], M. van Veghel[74], R. Vazquez Gomez[47], P. Vazquez Regueiro[45], C. Vázquez Sierra[31], S. Vecchi[20], J. J. Velthuis[53], M. Veltri[21,r], A. Venkateswaran[67], M. Vernet[9], M. Veronesi[31], M. Vesterinen[55], J. V. Viana Barbosa[47], D. Vieira[5], M. Vieites Diaz[48], H. Viemann[73], X. Vilasis-Cardona[44], A. Vitkovskiy[31], A. Vollhardt[49], D. Vom Bruch[12], B. Voneki[47], A. Vorobyev[37], V. Vorobyev[42,x], N. Voropaev[37], R. Waldi[73], J. Walsh[28], J. Wang[3], J. Wang[71], J. Wang[6], M. Wang[3], Y. Wang[7], Z. Wang[49], D. R. Ward[54], H. M. Wark[59], N. K. Watson[52], D. Websdale[60], A. Weiden[49], C. Weisser[63], B. D. C. Westhenry[53], D. J. White[61], M. Whitehead[13], D. Wiedner[14], G. Wilkinson[62], M. Wilkinson[67], I. Williams[54], M. Williams[63], M. R. J. Williams[61], T. Williams[52], F. F. Wilson[56], M. Winn[11], W. Wislicki[35], M. Witek[33], L. Witola[16], G. Wormser[11], S. A. Wotton[54], H. Wu[67], K. Wyllie[47], Z. Xiang[5], D. Xiao[7], Y. Xie[7], H. Xing[70], A. Xu[3], J. Xu[5], L. Xu[3], M. Xu[7], Q. Xu[5], Z. Xu[8], Z. Xu[3], Z. Yang[3], Z. Yang[65], Y. Yao[67], L. E. Yeomans[59], H. Yin[7], J. Yu[7,z], X. Yuan[67], O. Yushchenko[43], K. A. Zarebski[52], M. Zavertyaev[15,c], M. Zdybal[33], M. Zeng[3], D. Zhang[7], L. Zhang[3], S. Zhang[3], W. C. Zhang[3], Y. Zhang[47], A. Zhelezov[16], Y. Zheng[5], X. Zhou[5], Y. Zhou[5], X. Zhu[3], V. Zhukov[13,39], J. B. Zonneveld[57], S. Zucchelli[19,e]

[1] Centro Brasileiro de Pesquisas Físicas (CBPF), Rio de Janeiro, Brazil
[2] Universidade Federal do Rio de Janeiro (UFRJ), Rio de Janeiro, Brazil
[3] Center for High Energy Physics, Tsinghua University, Beijing, China
[4] School of Physics State Key Laboratory of Nuclear Physics and Technology, Peking University, Beijing, China
[5] University of Chinese Academy of Sciences, Beijing, China
[6] Institute Of High Energy Physics (IHEP), Beijing, China
[7] Institute of Particle Physics, Central China Normal University, Wuhan, Hubei, China
[8] Univ. Grenoble Alpes, Univ. Savoie Mont Blanc, CNRS, IN2P3-LAPP, Annecy, France
[9] Université Clermont Auvergne, CNRS/IN2P3, LPC, Clermont-Ferrand, France
[10] Aix Marseille Univ, CNRS/IN2P3, CPPM, Marseille, France
[11] Université Paris-Saclay, CNRS/IN2P3, IJCLab, Orsay, France
[12] LPNHE, Sorbonne Université, Paris Diderot Sorbonne Paris Cité, CNRS/IN2P3, Paris, France
[13] I. Physikalisches Institut, RWTH Aachen University, Aachen, Germany
[14] Fakultät Physik, Technische Universität Dortmund, Dortmund, Germany
[15] Max-Planck-Institut für Kernphysik (MPIK), Heidelberg, Germany
[16] Physikalisches Institut, Ruprecht-Karls-Universität Heidelberg, Heidelberg, Germany
[17] School of Physics, University College Dublin, Dublin, Ireland
[18] INFN Sezione di Bari, Bari, Italy
[19] INFN Sezione di Bologna, Bologna, Italy
[20] INFN Sezione di Ferrara, Ferrara, Italy
[21] INFN Sezione di Firenze, Florence, Italy
[22] INFN Laboratori Nazionali di Frascati, Frascati, Italy
[23] INFN Sezione di Genova, Genoa, Italy
[24] INFN Sezione di Milano-Bicocca, Milan, Italy
[25] INFN Sezione di Milano, Milan, Italy
[26] INFN Sezione di Cagliari, Monserrato, Italy
[27] INFN Sezione di Padova, Padua, Italy
[28] INFN Sezione di Pisa, Pisa, Italy
[29] INFN Sezione di Roma Tor Vergata, Rome, Italy
[30] INFN Sezione di Roma La Sapienza, Rome, Italy
[31] Nikhef National Institute for Subatomic Physics, Amsterdam, The Netherlands
[32] Nikhef National Institute for Subatomic Physics and VU University Amsterdam, Amsterdam, The Netherlands

[33] Henryk Niewodniczanski Institute of Nuclear Physics Polish Academy of Sciences, Kraków, Poland
[34] Faculty of Physics and Applied Computer Science, AGH-University of Science and Technology, Kraków, Poland
[35] National Center for Nuclear Research (NCBJ), Warsaw, Poland
[36] Horia Hulubei National Institute of Physics and Nuclear Engineering, Bucharest-Magurele, Romania
[37] Petersburg Nuclear Physics Institute NRC Kurchatov Institute (PNPI NRC KI), Gatchina, Russia
[38] Institute of Theoretical and Experimental Physics NRC Kurchatov Institute (ITEP NRC KI), Moscow, Russia
[39] Institute of Nuclear Physics, Moscow State University (SINP MSU), Moscow, Russia
[40] Institute for Nuclear Research of the Russian Academy of Sciences (INR RAS), Moscow, Russia
[41] Yandex School of Data Analysis, Moscow, Russia
[42] Budker Institute of Nuclear Physics (SB RAS), Novosibirsk, Russia
[43] Institute for High Energy Physics NRC Kurchatov Institute (IHEP NRC KI), Protvino, Russia
[44] ICCUB, Universitat de Barcelona, Barcelona, Spain
[45] Instituto Galego de Física de Altas Enerxías (IGFAE), Universidade de Santiago de Compostela, Santiago de Compostela, Spain
[46] Instituto de Fisica Corpuscular, Centro Mixto Universidad de Valencia-CSIC, Valencia, Spain
[47] European Organization for Nuclear Research (CERN), Geneva, Switzerland
[48] Institute of Physics, Ecole Polytechnique Fédérale de Lausanne (EPFL), Lausanne, Switzerland
[49] Physik-Institut, Universität Zürich, Zurich, Switzerland
[50] NSC Kharkiv Institute of Physics and Technology (NSC KIPT), Kharkiv, Ukraine
[51] Institute for Nuclear Research of the National Academy of Sciences (KINR), Kiev, Ukraine
[52] University of Birmingham, Birmingham, UK
[53] H.H. Wills Physics Laboratory, University of Bristol, Bristol, UK
[54] Cavendish Laboratory, University of Cambridge, Cambridge, UK
[55] Department of Physics, University of Warwick, Coventry, UK
[56] STFC Rutherford Appleton Laboratory, Didcot, UK
[57] School of Physics and Astronomy, University of Edinburgh, Edinburgh, UK
[58] School of Physics and Astronomy, University of Glasgow, Glasgow, UK
[59] Oliver Lodge Laboratory, University of Liverpool, Liverpool, UK
[60] Imperial College London, London, UK
[61] Department of Physics and Astronomy, University of Manchester, Manchester, UK
[62] Department of Physics, University of Oxford, Oxford, UK
[63] Massachusetts Institute of Technology, Cambridge, MA, USA
[64] University of Cincinnati, Cincinnati, OH, USA
[65] University of Maryland, College Park, MD, USA
[66] Los Alamos National Laboratory (LANL), Los Alamos, USA
[67] Syracuse University, Syracuse, NY, USA
[68] Laboratory of Mathematical and Subatomic Physics , Constantine, Algeria, associated to [2]
[69] Pontifícia Universidade Católica do Rio de Janeiro (PUC-Rio), Rio de Janeiro, Brazil, associated to [2]
[70] Guangdong Provincial Key Laboratory of Nuclear Science, Institute of Quantum Matter, South China Normal University, Guangzhou, China, associated to [3]
[71] School of Physics and Technology, Wuhan University, Wuhan, China, associated to [3]
[72] Departamento de Fisica, Universidad Nacional de Colombia, Bogotá, Colombia, associated to [12]
[73] Institut für Physik, Universität Rostock, Rostock, Germany, associated to [16]
[74] Van Swinderen Institute, University of Groningen, Groningen, The Netherlands, associated to [31]
[75] National Research Centre Kurchatov Institute, Moscow, Russia, associated to [38]
[76] National University of Science and Technology "MISIS", Moscow, Russia, associated to [38]
[77] National Research University Higher School of Economics, Moscow, Russia, associated to [41]
[78] National Research Tomsk Polytechnic University, Tomsk, Russia, associated to [38]
[79] University of Michigan, Ann Arbor, USA, associated to [67]

[a] Universidade Federal do Triângulo Mineiro (UFTM), Uberaba-MG, Brazil
[b] Laboratoire Leprince-Ringuet, Palaiseau, France
[c] P.N. Lebedev Physical Institute, Russian Academy of Science (LPI RAS), Moscow, Russia

[d] Università di Bari, Bari, Italy
[e] Università di Bologna, Bologna, Italy
[f] Università di Cagliari, Cagliari, Italy
[g] Università di Ferrara, Ferrara, Italy
[h] Università di Genova, Genoa, Italy
[i] Università di Milano Bicocca, Milan, Italy
[j] Università di Roma Tor Vergata, Rome, Italy
[k] Università di Roma La Sapienza, Rome, Italy
[l] AGH-University of Science and Technology, Faculty of Computer Science, Electronics and Telecommunications, Kraków, Poland
[m] DS4DS, La Salle, Universitat Ramon Llull, Barcelona, Spain
[n] Hanoi University of Science, Hanoi, Vietnam
[o] Università di Padova, Padua, Italy
[p] Università di Pisa, Pisa, Italy
[q] Università degli Studi di Milano, Milan, Italy
[r] Università di Urbino, Urbino, Italy
[s] Università della Basilicata, Potenza, Italy
[t] Scuola Normale Superiore, Pisa, Italy
[u] Università di Modena e Reggio Emilia, Modena, Italy
[v] Università di Siena, Siena, Italy
[w] MSU - Iligan Institute of Technology (MSU-IIT), Iligan, Philippines
[x] Novosibirsk State University, Novosibirsk, Russia
[y] INFN Sezione di Trieste, Trieste, Italy
[z] Physics and Micro Electronic College, Hunan University, Changsha City, China
[†] Deceased